PROF. OWEN K ATKIN (Orcid ID : 0000-0003-1041-5202)

Article type : MS - Regular Manuscript

The validity of optimal leaf traits modelled on environmental conditions

Keith J. Bloomfield[*1], I. Colin Prentice[2,3], Lucas A. Cernusak[4], Derek Eamus[5], Belinda E. Medlyn[6], Rizwana Rumman[5], Ian J. Wright[2], Matthias M. Boer[6], Peter Cale[7], James Cleverly[5,8], John J.G. Egerton[1], David S. Ellsworth[6], Bradley J. Evans[9], Lucy S. Hayes[1], Michael F. Hutchinson[10], Michael J. Liddell[11], Craig Macfarlane[12], Wayne S. Meyer[13], Henrique F. Togashi[2], Tim Wardlaw[14], Lingling Zhu[1,15] and Owen K. Atkin[1,15]

[1]Division of Plant Sciences, Research School of Biology, Building 46, The Australian National University, Canberra, ACT 2601, Australia; [2]Department of Biological Sciences, Macquarie University, North Ryde, NSW 2109, Australia; [3]AXA Chair of Biosphere and Climate Impacts, Grand Challenges in Ecosystems and the Environment and Grantham Institute—Climate Change and the Environment, Department of Life Sciences, Imperial College London, Silwood Park Campus, Buckhurst Road, Ascot SL5 7PY, UK; [4]Department of Marine and Tropical Biology, James Cook University, Cairns, Qld 4878, Australia; [5]School of Life Sciences, University of Technology Sydney, NSW 2007, Australia; [6]Hawkesbury Institute for the Environment, Western Sydney University, Penrith, NSW 2751, Australia; [7]Australian Landscape Trust, Renmark, SA 5341, Australia; [8]TERN (Terrestrial Ecosystem Research Network, University of Technology Sydney); [9]Faculty of Agriculture and Environment, Department of Environmental Sciences, University of Sydney, Sydney, NSW 2006, Australia; [10]Fenner School

of Environment and Society, Australian National University, Canberra, ACT 2601, Australia; [11]Centre for Tropical, Environmental, and Sustainability Sciences, James Cook University, Cairns, Qld, Australia; [12]CSIRO Land and Water, Private Bag 5, Wembley, WA 6913, Australia; [13]Earth and Environmental Sciences, University of Adelaide, Adelaide, SA 5064, Australia; [14]ARC Centre for Forest Value, University of Tasmania, Hobart, TAS 7005, Australia; [15]ARC Centre of Excellence in Plant Energy Biology, Research School of Biology, Building 134, The Australian National University, Canberra, ACT 2601, Australia.

* Corresponding author: Keith.Bloomfield@anu.edu.au

Tel: +44 28 71341685

Received: 28 July 2018

Accepted: 7 September 2018

Lucas Cernusak 0000-0002-7575-5526

James Cleverly 0000-0002-2731-7150

Derek Eamus 0000-0003-2765-8040

Ian Wright 0000-0001-8338-9143

Summary

- The ratio of leaf intercellular to ambient CO_2 (χ) is modulated by stomatal conductance (g_s). These quantities link carbon (C) assimilation with transpiration, and along with photosynthetic capacities (V_{cmax} and J_{max}) are required to model terrestrial C uptake. We use optimisation criteria based on the growth environment to generate predicted values of photosynthetic and water-use efficiency traits and test these against a unique dataset.
- Leaf gas-exchange parameters and carbon isotope discrimination were analysed in relation to local climate across a continental network of study sites. Sun-exposed leaves of 50 species at seven sites were measured in contrasting seasons.

- Values of χ predicted from growth temperature and vapour pressure deficit were closely correlated to ratios derived from C isotope ($\delta^{13}C$) measurements. Correlations were stronger in the growing season. Predicted values of photosynthetic traits, including carboxylation capacity (V_{cmax}), derived from $\delta^{13}C$, growth temperature and solar radiation, showed meaningful agreement with inferred values derived from gas-exchange measurements. Between-site differences in water use efficiency were, however, only weakly linked to the plant's growth environment and did not show seasonal variation.
- These results support the general hypothesis that many key parameters required by Earth system models are adaptive and predictable from plants' growth environments.

Keywords:
aridity, photosynthesis, stable isotopes, stomatal conductance (g_s), temperature, water-use efficiency.

Introduction

All healthy leaves ultimately fulfil the same functions of light capture and gas exchange. In C_3 plants, the ratio (χ) of leaf intercellular (C_i) to ambient (C_a) partial pressure of CO_2 depends on a balance between stomatal conductance (g_s) and photosynthesis, which in turn depends on C_i, on leaf-level capacities for carboxylation (V_{cmax}) and electron transport (J_{max}), and on temperature-dependent kinetic constants. We can have confidence in our ability to measure and monitor C_a, but knowledge of associated C_i - made possible by reliable estimates of χ - is crucial to understanding the leaf's carbon economy. There are large variations in χ, g_s, V_{cmax} and J_{max} across species and environments (Schulze *et al.*, 1994; De Kauwe *et al.*, 2016; Wang *et al.*, 2017b). Faced with huge global diversity in plant species (and the morphology, physiology and longevity of leaves) there is great benefit in quantifying unifying trends that may be widely applied in global-scale models. The worldwide leaf economics spectrum (LES) is a notable example (Wright *et al.*, 2004), most importantly describing a trade-off between specific leaf area (the ratio of leaf area to dry mass) and leaf longevity. Considerable variation in the gas exchange parameters listed above is, however, unrelated to the LES. Given the fundamental importance of these parameters for modelling land-atmosphere carbon and water exchange, it is vital that tools be developed to predict variations in χ, g_s, V_{cmax} and J_{max}.

Current models of vegetation and land-surface processes, including those embedded in Earth system models (ESMs), typically prescribe values of V_{cmax} and J_{max} for each plant functional type (PFT) and use empirical models to predict χ and g_s. This approach has major limitations because (a) there is at least as much variation in V_{cmax} and J_{max} within as among PFTs (e.g. Verheijen *et al.*, 2013; Rogers, 2014) and (b) the empirical models require the specification of further parameters for PFTs. An alternative approach is to seek general functional relationships that allow these photosynthetic parameters to be predicted from environmental information (Reich *et al.*, 2007; Ali *et al.*, 2015). A promising route to defining such relationships is provided by optimality hypotheses, couched in quantitative terms that allow testing against field measurements (Mäkelä *et al.*, 2002; Prentice *et al.*, 2014; Prentice *et al.*, 2015). There is a need to test the predictions emanating from such models against empirical data drawn from as wide as possible a range of natural settings.

To balance water loss against carbon gain, the plant must control g_s which modulates both rates. When stomata are open, the leaf-to-air vapour pressure deficit (D) provides the gradient that drives transpiration (E). Ratios of carbon assimilation (A) to E, provide one measure of the plant's water use efficiency (WUE) and for C_3 plants vary from 2 to 11 mmol C mol^{-1} H_2O (Lambers *et al.*, 2008), illustrating the high water cost of C gain. Cowan and Farquhar (1977) introduced an optimality hypothesis for stomatal regulation, defining a parameter λ that may be thought of as an exchange rate between water and C. Their hypothesis proposes that, over the course of a single day, optimal stomatal behaviour minimises E for a given A such that the relative sensitivities of E and A to changes in g_s remain constant:

$$\frac{\partial E/\partial gs}{\partial A/\partial gs} = \frac{\partial E}{\partial A} = \lambda \qquad (1)$$

Cowan and Farquhar pointed out that this exchange rate must vary with ontogeny and changing environment – no single value could be appropriate at all life stages and under all conditions. Subsequent controlled-environment studies across a range of tree species have confirmed that estimated values of λ, derived from empirical models, vary with leaf temperature (T), D, irradiance, soil water content and atmospheric pressure (Lloyd, 1991; Thomas *et al.*, 1999; Wang *et al.*, 2017a). But as λ is not directly measurable, Eqn 1 lacks useful predictive power over time scales longer than the diurnal cycle. In consequence, it has not been adopted in models, which instead typically constrain g_s using the empirical observations of a strong positive correlation with A (Wong *et al.*, 1979) and a strong negative response to D.

Recent studies have attempted to combine theoretical and empirical approaches. Medlyn *et al.* (2011) presented a unified model of optimal stomatal conductance (g_s^*):

$$g_s^* \approx g_0 + 1.6\left(1 + \frac{g_1}{\sqrt{D}}\right)\frac{A}{C_a} \quad (2)$$

where g_0 and g_1 are parameters that can be estimated using gas-exchange measurements with varying D. Eqn 2 is an approximate solution of Eqn 1 under electron-transport limitation of photosynthesis (adopted on the grounds that guard cells controlling stomatal aperture have markedly greater capacity for electron transport than for Rubisco C fixation) (Medlyn *et al.*, 2011). The model's slope parameter g_1 is proportional to the product of λ and the photorespiratory CO_2 compensation point (Γ^*). The value of g_1 was found empirically to vary among PFTs and to increase with growth temperature in line with the increase in Γ^* (Medlyn *et al.*, 2011; Lin *et al.*, 2015). In a parallel result obtained by Katul *et al.* (2010) for Rubisco-limited photosynthesis, optimal stomatal behaviour described by Eqn 1 yields a similar response to D but a different response to C_a (see discussion by Medlyn *et al.*, 2013).

From a modelling perspective, however, the chief difficulty with Eqn 2 is that we have no *a priori* derivation of the parameter values g_0 and g_1. Several alternatives to the Cowan-Farquhar hypothesis have been proposed, but because rates of A and E respond independently to so many variables a fully mechanistic understanding of the costs of stomatal opening is still lacking (Dewar *et al.*, 2018). Sperry *et al.* (2016) and Wolf *et al.* (2016) considered an optimization criterion whereby an explicit carbon cost is assigned to the risk of hydraulic failure associated with water transport. Wolf *et al.* (2016) further critiqued the Cowan-Farquhar criterion on theoretical grounds, as its implicit water cost is based on the loss of water from a store shared by all plants – ignoring competition between plants for the same water violates the criterion for an evolutionarily stable strategy. Prentice *et al.* (2014) introduced an optimization criterion that assigns explicit carbon costs to the maintenance capacities for both water transport and carboxylation, and assumes that plants minimize the fraction of assimilation assigned to the sum of these costs. This criterion leads to an optimal value of χ (χ_o):

$$\chi_o \approx \frac{\xi}{(\xi + \sqrt{D})} \text{ with } \xi = \sqrt{\left(\frac{bK}{1.6a}\right)} \quad (3)$$

where K is the effective Michaelis-Menten coefficient of Rubisco (i.e. reflecting the enzyme's twin affinities for CO_2 and O_2), and a and b are empirical cost factors for water transport and carboxylation respectively. Mathematically, equation (3) has a similar form to Eqn 2. If g_0 in

Eqn 2 is ignored, re-arrangement yields the same optimal value of χ as Eqn 3 with $\xi = g_1$. But importantly ξ (again a parameter related to the water cost of carbon gain) now depends on K rather than Γ^*, and the term λ has been replaced by the ratio b/a, which can be estimated empirically from instantaneous gas exchange measurements (as in Lin *et al.*, 2015) or stable carbon isotope ratios ($\delta^{13}C$). χ_o increases with T because of the temperature-dependency of K (Bernacchi *et al.*, 2001) and because the viscosity of water has an inverse relationship with T, so that the cost factor for water transport (a) decreases with T (Prentice *et al.*, 2014). Wang *et al.* (2017b) showed that χ_o is a function of growth D, T and altitude (z) (Wang *et al.*, 2017a) and can be represented in a linearized form around $T = 25^\circ C$ as follows:

$$\ln[\chi_o/(1-\chi_o)] = 1.189 + 0.0545\,(T-25) - 0.5\ln D - 0.0815\,z \qquad (4)$$

in which the constant 1.189 (dependent on b/a) was estimated from a large global set of $\delta^{13}C$ measurements, while the predicted coefficients of $(T - 25)$, $\ln D$ and z in equation (4) lay within confidence intervals estimated empirically from the $\delta^{13}C$ dataset. Under standard growth conditions ($T = 25°C$, $D = 1$ kPa, $z = 0$ m), Eqn 4 yields $\chi_o = 0.77$ and this value decreases with D, increases with T, and decreases with z.

Eqn 4 provides testable predictions of χ, and therefore of C_i. But to predict A using the standard biochemical model of C_3 photosynthesis (Farquhar *et al.*, 1980; the FvCB model) as generally employed in ESMs, we also need to know the carboxylation capacity (V_{cmax}) and the rate of electron transport (J). Here we introduce another long-standing optimality hypothesis, the co-limitation or co-ordination hypothesis (e.g. Chen *et al.*, 1993; Maire *et al.*, 2012), which states that the two limiting rates of photosynthesis tend toward equality under average daytime conditions. By equating these two co-limiting photosynthetic rates and making the simplifying assumption that J is proportional to photosynthetically active radiation (PAR) absorbed by the leaf (I_L), Dong *et al.* (2017) derived an approximation of optimal V_{cmax}:

$$V_{cmax} \approx \varphi_0 I_L \frac{(C_i + K)}{(C_i + 2\Gamma^*)} \qquad (5)$$

where φ_0 is the intrinsic quantum efficiency of photosynthesis, here taken to equal 0.085 (Collatz *et al.*, 1991). The description of the leaf light term (I_L) is given in Methods (below). Pursuing the co-ordination hypothesis further, the ratio of the rate of maximal electron transport (J_{max}) to V_{cmax} also points to investment strategies within the leaf (Poorter & Evans, 1998) that

may in turn be influenced by the environmental conditions experienced by the plant. Further derivations in Wang *et al.* (2017b) yield an optimal ratio:

$$\frac{J_{max}}{V_{cmax}} = \frac{4}{(C_i + K)} \cdot \sqrt[3]{\frac{(C_i - \Gamma^*) \cdot (C_i + 2\Gamma^*)^2}{0.41}} \quad (6)$$

where the constant 0.41 was estimated by assuming that typical values for the ratios J_{max}/V_{cmax} (1.88) and χ (0.8) correspond with standard growth conditions (see references in Wang *et al.*).

In the current study, by employing independent methods for estimating the leaf's C_i, we set out to test the validity of these foregoing predictions. In seeking to validate the models explicitly related to stomatal behaviour (parameters g_1 and χ), we focus on the estimates derived using time-averaged data ($\delta^{13}C$ rather than instantaneous gas exchange) as the more useful test for dynamic vegetation models on similar grounds to those proposed above, arguing that a constant λ is infeasible. We present a unique Australian dataset that combines leaf gas-exchange measurements with concurrent, site-based meteorological data and foliar carbon isotope analysis. The dataset comprises 50 plant species growing at seven environmentally contrasting sites, with repeat measurements taken in contrasting seasons. We used these data to address the following questions:

1. How well do instantaneous (gas-exchange) and time-averaged (isotope) measures of optimal stomatal behaviour agree?
2. Do the predictions of the unified stomatal model represented by Eqn 2 help to reveal spatial and seasonal patterns of leaf water use efficiency?
3. Can temporal variation in the integrated C_i/C_a ratio, as indexed by $\delta^{13}C$ measurements, be predicted from growth temperature and vapour pressure deficit as indicated by Eqn 4?
4. How well do predictions of V_{cmax}, and the ratio J_{max}/V_{cmax}, derived under the co-ordination hypothesis following Eqns 5 and 6 correlate to independent gas-exchange measurements?

Methods

Study sites and climate data

Our seven study sites are a subset of TERN Ecosystem Processes 'SuperSites' (supersites.tern.org.au) (Karan *et al.*, 2016). TERN Ecosystem Processes is a platform of the Terrestrial Ecosystem Research Network (TERN), Australia's land–ecosystem observatory. Site locations and key descriptors of dominant vegetation and soil type are presented in Table 1. The sites were chosen to provide a wide range of environmental conditions (Supporting Information Fig. S1). Each SuperSite is equipped with a flux tower (TERN OzFlux) that records a common suite of meteorological data (Beringer *et al.*, 2016). Our initial visits pre-dated the installation of the standard OzFlux system at three sites; in those instances we used the ANUClimate statistical model (Hutchinson *et al.*, 2009) and data from the Australian Bureau of Meteorology's nearest weather station (TERN eMAST). The proportion of down-welling shortwave radiation (Fsd, OzFlux) deemed as PAR was 0.47 (Britton & Dodd, 1976).

Apart from Alice Mulga, each site was visited twice. The timing of the visits was designed, within logistical constraints, to provide the widest possible seasonal contrast. The prevailing climate conditions leading up to each campaign are provided in Table 2. In testing for environmental dependencies of leaf traits, we considered a range of time-periods. In a glasshouse experiment on different *Nothofagus* species, Read & Farquhar (1991) found that for Australasian species the environmental parameter of the collection site most closely correlated with genetically determined C isotope discrimination (Δ) was the precipitation from the period December to March. Our study of leaf traits included seasonal contrasts (i.e. sub-annual) and so an intermediate (quarterly) time step has been adopted to represent average environmental conditions. Model iterations (e.g. Eqns 4 and 5) were run also adopting weekly and monthly time-steps, but offered neither improved explanatory power nor qualitative changes to the results (data not shown).

Leaf gas exchange

The plants measured (50 species, Supporting Information Table S1), were selected to include locally dominant species of trees and shrubs. This is a subset (combined here with C isotope analysis) of a larger dataset presented in Bloomfield *et al.* (2018). At each visit, we chose young, fully developed leaves from two sun-exposed branches. Leaf gas exchange measurements were concentrated in the morning and performed using portable photosynthesis systems (Li-Cor 6400, Li-Cor, Lincoln, NE, USA), using the 6 cm^2 chamber fitted with the red-blue light source (Li-

Cor 6400-02B LED). Upper canopy branches were excised using forestry shears on telescopic poles and the branches immediately placed in a bucket and the branches recut under water to re-establish the xylem water column (Domingues *et al.*, 2010). Performing gas-exchange measurements on excised branches can affect subsequent calculations where stomatal conductance is heavily depressed. Our initial data exploration excluded such outliers (36 rows for individual leaves, 3.2% of the dataset).

For each leaf, approximately light-saturated (1500 μmol photons m^{-2} s^{-1}) measures of net photosynthesis were taken at two CO_2 concentrations: 400 μmol mol^{-1} (ppm) (A_{400}) and 1500 μmol mol^{-1} (A_{1500}). The leaf was next wrapped in aluminium foil for 30 minutes before respiration in darkness (R_{dark}) was measured, still at 400 ppm CO_2. Air flow was held constant and a constant chamber block temperature (T_{Block}) was adopted for all measurements at a given site and season, set marginally (≈ 1°C) higher than expected morning air temperatures to counter the effect of transpirational cooling and ensure leaf and ambient air temperatures were similar. T_{Block} settings ranged from 10°C for the winter visit to Warra to 32°C for the summer visit to Calperum, reflecting the wide range of air temperatures experienced across the sites and seasons. The Li-Cor 6400 system can maintain T_{Block} values ±6°C away from ambient and this operating constraint precluded measuring gas exchange at a common temperature across all sites and seasons. With a constant flow rate, chamber humidity conditions varied and mean *D* within the chamber ranged from 0.55 kPa for the winter visit to Warra to 4.02 kPa for the summer visit to Calperum.

In the absence of *A*-C_i response curves, we estimated V_{cmax} based on our light-saturated A_{400} values using the 'one-point method' described and validated by de Kauwe *et al.* (2016). Mitochondrial respiration in the light (R_{day}) was assumed to be equivalent to R_{dark} (this simplifying assumption has only a very minor effect on the estimation of V_{cmax}). The rate of electron transport at saturating [CO_2] of 1500 ppm (J_{max}) was estimated according to the equation:

$$J_{max} = (A_{1500} + R_{dark}) \cdot \frac{(4C_i + 8\Gamma^*)}{(C_i - \Gamma^*)} \quad (7)$$

Our estimates of V_{cmax} and J_{max} reflect temperature dependencies applied to *K* and Γ^* according to Bernacchi *et al.* (2001). To allow comparisons of metabolic rates across sites and seasons, we calculated rates at both a standard temperature (25°C) and at the average daytime air temperature for the 90-day period leading up to the end of each field campaign (Table 2). From the rate derived at a given measurement temperature, normalised V_{cmax} was calculated by applying the

Arrhenius function (Medlyn *et al.*, 2002) assuming an activation energy of 64.8 kJ mol^{-1} (Badger & Collatz, 1977).

Photosynthetic model extensions

When modeling V_{cmax} (Eqn 5), we adopted a simple leaf light term (I_L):

$$I_L \approx I_0 \frac{\left(1 - e^{-k\,LAI}\right)}{LAI} \quad (8)$$

that estimates mean canopy light availability based on leaf area index (LAI) in the plot, where I_0 is incident PAR at the top of the canopy and k is an extinction coefficient. We have assumed k = 0.5 since even distal leaves on sun-exposed branches usually experience only a fraction of full PAR incident at the horizontal plane (e.g. Kitajima *et al.*, 2005). As LAI approaches zero, the I_L term's upper limit is $I_0/2$, but becomes a diminishing fraction of I_0 as canopy density increases. Even though our sampling protocol called for sun-exposed leaves, we consider that adopting I_0 would overestimate PAR for many mid-canopy or understory species.

The FvCB model and its subsequent implementations make the simplifying assumption for C_3 plants that CO_2 conductance through the leaf's mesophyll (g_m) is infinite such that the partial pressure at the site of carboxylation in the chloroplast (C_c) is equal to C_i. It is known, however, that internal resistances can lower g_m and Evans & von Caemmerer (1996) reported that for many species C_c may be around 30% lower than C_i when leaves are actively photosynthesising in high light. Variations in g_m are potentially important in a study such as ours that includes measurements of plants growing at environmentally contrasting sites and at unfavourable seasons. Following the approach in Ayub *et al.* (2011) we estimated g_m based on the strong empirical correlation with A_{sat} presented in Evans & von Caemmerer (1996), but adopting a drawdown (sub-stomatal airspace to chloroplasts: A/g_m) of 50 μmol mol^{-1} suggested as a lower bound in a subsequent meta-analysis by Niinemets *et al.* (2009). C_c was then derived according to:

$$C_c = C_i - \frac{A_{sat}}{g_m} = C_i - 50 \quad (9)$$

Photosynthetic parameters inferred from gas exchange measurements ('one point' estimates of V_{cmax}; J_{max} according to Eqn 7) are presented in the analysis that follows after substituting C_c for C_i and adopting lowered Michaelis constants for Rubisco's carboxylation and oxygenation reactions after von Caemmerer *et al.* (1994). Dropping the assumption of infinite g_m, Wang *et al.*

(2017b) derived a modified equation for χ_c with unchanged environmental dependencies, but producing a lower constant of 1.097 (replacing the 1.189 intercept term in Eqn 4) reflecting the anticipated drawdown from C_i to C_c i.e. $\chi_c < \chi_o$.

Estimating χ from stable carbon isotope discrimination

As an alternative to instantaneous methods, χ can be inferred from the leaf's stable isotope composition. In their uptake of atmospheric CO_2, plants discriminate against the stable ^{13}C isotope relative to the lighter, more abundant ^{12}C isotope and the level of discrimination is influenced by environmental conditions (Farquhar *et al.*, 1989). Isotopic discrimination (Δ) can thus be expressed as the $^{13}C/^{12}C$ isotope ratio ($\delta^{13}C$) of leaf tissue relative to that of source air. We here employ the simple model developed by Farquhar *et al.* (1982) whereby discrimination is given by:

$$\Delta\ (‰) = \frac{\delta^{13}C_a - \delta^{13}C_l}{1 + \delta^{13}C_l/1000} \quad (10)$$

where $\delta^{13}C_a$ is the $\delta^{13}C$ value of CO_2 in air (assumed to be -8‰) and $\delta^{13}C_l$ is that of the leaf. It is then possible to derive time-averaged values of χ (weighted for photosynthetically active periods) based on the relationship with Δ according to:

$$\chi = \frac{(\Delta - a')}{(b' - a')} \quad (11)$$

where a' is the isotope fractionation arising from diffusion through the stomata and b' the net fractionation caused by carboxylation, with standard values for C_3 plants of 4.4‰ and 27‰ respectively. Eqn 11 is an approximation and disregards a number of additional dependencies of $\delta^{13}C$ (e.g. Ubierna & Farquhar, 2014), but works well in practice because the generally adopted value of *b'* implicitly includes these effects (Cernusak *et al.*, 2013). An extended formulation that included explicit fractionation terms for mesophyll transfer and photorespiration was presented by Seibt *et al.* (2008). We here extend their 'classical' model to include a term presented by Farquhar & Cernusak (2012) that corrects the isotopic estimates of C_i for the effects of transpiration on the diffusive flux of CO_2 already captured in the LiCor formulation – the ternary factor (so called to describe the collision of molecules of CO_2, water vapour and air). Solving for χ provides a revised ratio:

$$\chi = \frac{\Delta(1-t) - a' + (b - a_m)(1+t)\frac{A}{g_m C_a} + (1+t) f \frac{\Gamma^*}{C_a}}{(b + tb - a')} \quad (12)$$

where $t = \frac{E}{2\frac{g_s}{1.6}}$

is the ternary correction factor, b is the mean fractionation during carboxylation by Rubisco (30‰), a_m is fractionation during transfer through the mesophyll (1.1‰) and f is fractionation during photorespiration (8‰). Hereafter we distinguish between these two discrimination models by referring to the simple (Eqn 11) and neo-classical (Eqn 12) formulations.

$\delta^{13}C$ methods, conducted on leaves sampled from the same branch as gas exchange measurements, are as described in Rumman *et al.* (2018). Briefly, after drying each leaf sample was finely ground until homogenous with a ball mill (Retsch MM300, Verder Group, Netherlands). Between one and two milligrams of ground material were sub-sampled in tin capsules for analysis of $\delta^{13}C$, giving three representative values per tree. All $\delta^{13}C$ analyses were performed using a Picarro G2121-i Analyser (Picarro, Santa Clara, CA, USA) for isotopic CO_2. Atropine and acetanilide were used as laboratory standard references and results were normalised with the international standards sucrose (IAEA-CH-6, $\delta^{13}C_{VPDB}$ = –10.45 ‰), cellulose (IAEA-CH-3, $\delta^{13}C_{VPDB}$ = –24.72 ‰) and graphite (USGS24, $\delta^{13}C_{VPDB}$ = –16.05 ‰). Standard deviation of the residuals between the IAEA standards and the calculated values of $\delta^{13}C$ based on best linear fit was ≈ 0.5 ‰.

Estimating g_1

The value of $g_{1\text{-leaf}}$ was estimated by fitting the unified stomatal model (Eqn 2) to our leaf gas exchange data using the fitBB function in the *plantecophys* R package (Duursma, 2015); gas exchange data for input to the model were restricted here to the A_{400} measurements described above. Values of isotope-derived g_1 were estimated following Medlyn *et al.* (2011) using χ values obtained from Eqn 12 according to

$$g_{1-isotope} = \frac{(\chi\sqrt{D})}{(1-\chi)} \quad (13)$$

where D relates to time-averaged daylight site values obtained from the OzFlux network.

Data analysis

All statistical analyses were conducted using the open-sourced statistical environment 'R' (R Development Core Team, 2017). Leaf trait and parameter observations are presented as species averages for a given site and season; sample size and standard deviations are given in Supporting Information (Table S2). The level of agreement between two independent measures of a trait, or between model predictions and independently measured trait values, was tested using Pearson correlations. Linear mixed effects models, from the *nlme* package (Pinheiro *et al.*, 2018), were used to test for differences between sites and seasons for the g_1 parameter and for relationships between isotope-derived χ and the environmental variables T and D; a common random effect allowed different intercepts for each plant family. Differences between sites were assigned using Tukey's honest significant differences (HSD). Comparisons between nested models were assessed using log likelihood ratios (L). Partial residual plots showing the relationship between independent parameter estimates and model explanatory variables were represented using the *visreg* R package (Breheny & Burchett, 2017).

Results

Stomatal behaviour

We found a positive, but weak correlation ($r = 0.290$) between our gas exchange- and isotope-derived versions of the g_1 slope parameter (Fig. 1) although for tropical forest species several of the isotope-derived values were unrealistically high (>20 $kPa^{0.5}$; corresponding to C_i/C_a ratios approaching unity). Instantaneous estimates of the C_i/C_a ratio within the Li-Cor chamber were consistently lower than the isotope-derived ratios, but the effect on $g_{1\text{-leaf}}$ was partially offset by higher D within the chamber at the time of measurement relative to the daytime mean D of the preceding quarter (Supporting Information Fig. S2). We found no seasonal differences in the species-averaged $g_{1\text{-isotope}}$ estimates (even when models were run for a non-tropical subset of the sites); stepwise deletions from a fully interactive Site x Season fixed term (Site + Season + Site:Season) confirmed that the parsimonious Site-only model performed just as well ($L = 11.82$, $df = 6$, $p = 0.066$). Wide variation among co-occurring species meant there were few differences between the study sites, but $g_{1\text{-isotope}}$ values for Warra were lower than for the tropical forests (Fig. 2).

The expected influence of environmental conditions on stomatal behaviour was only partially borne out. The $g_{1\_isotope}$ parameter showed a weak positive relationship with time-averaged air temperatures ($R^2 = 0.10$ Supporting Information Fig. S3), but was unrelated to available indices of water availability: precipitation, moisture index or top-layer soil water fraction (e.g. for a multiple regression style model, dropping the soil water term to leave temperature as the sole explanatory variable made little difference to the model's performance: $L = 1.29$, $df = 1$, $p = 0.257$). Despite the limited agreement between our two versions of the g_1 parameter similar patterns were observed for $g_{1\text{-leaf}}$ (gas-exchange): a Site-only model was again preferred ($L = 9.07$, $df = 6$, $p = 0.169$); inter-site differences here suggested a progression of arid < temperate < tropical forests (Fig. 2 inset); but relationships with environmental variables were tentative at best: T ($R^2 = 0.11$).

Leaf Ci:Ca ratio

Estimates of χ modelled as a function of environmental parameters T and D using Eqn 4 (for this Australian dataset, we have ignored the limited site differences in altitude) showed strong correlation ($r = 0.702$) with corresponding ratios derived from ^{13}C discrimination (Eqn 12) (Fig. 3); the correlation was stronger still when ratios for co-occurring species were expressed as a site mean ($r = 0.930$). The modelled ratios were, however, consistently lower and we next considered how well Eqn 4 described our Δ-derived ratios. The consistent offset from the published model meant that our isotopic data yielded a markedly higher intercept at standard conditions from that proposed by Wang *et al.* (2017b) - corresponding to χ=0.85 (*versus* 0.75); the slope of the T response did not differ significantly from the theoretical value, but the slope coefficient for D was more steeply negative (Table 3). Our result of consistently higher Δ-derived χ stems from the decision to adopt an expanded formula of ^{13}C fractionation; a comparison of neo-classical *versus* simple $\chi_{\text{-isotope}}$ confirms that, whilst very closely correlated, the ratios were always higher under the extended formulation (Supporting Information Fig. S4b).

The fit of the Δ-derived ratios to the environmental data was improved when the two seasons were treated separately. The independent effects of the model's two environmental parameters suggested a seasonal shift in relative explanatory power with $T>D$ in the favourable season, but that ranking reversed in the off-season linked to pronounced deficits at Calperum and GWW (Table 3, Fig. 4).

393 *Photosynthetic parameters*

394 The maximal rate of Rubisco carboxylation (V_{cmax}), modelled using Eqn 5 adopting C_i estimates
395 derived from ^{13}C discrimination, showed fair agreement with estimates inferred from gas-
396 exchange measurements when expressed at the prevailing measurement temperatures (r = 0.675,
397 Fig. 5a). It is noticeable, however, that for a given site and season the rates inferred from gas
398 exchange were much more variable than the modelled values, reflecting the model's use of
399 environmental variables common to all co-occurring species.

400 The V_{cmax} rates shown in Fig. 5a reflect enzyme kinetics at the prevailing temperatures for each
401 site and season: average daytime temperatures (Table 2) for the modelled rates and leaf
402 temperatures close to a corresponding T_{Block} for the gas exchange measurements. When rates
403 were expressed normalised to a standard temperature of 25°C, the correlation between inferred
404 and modelled values proved weaker (r = 0.348, Fig. 5b). This disparity was caused, in part at
405 least, by the respective temperature differentials from the 25°C reference: leaf temperatures in
406 the Li-Cor chamber (inferred rates) always exceeded the daytime air temperatures (modelled
407 rates) (Methods). The divergence between inferred and modelled normalised rates became
408 more pronounced as the temperature differential increased (Supporting Information Fig. S5).
409 Once normalised for average canopy light conditions (I_L above), our 25°C standardised gas
410 exchange rates showed a negative relationship with growth temperature (Supporting Information
411 Fig. S6).

412 The modelled ratio J_{max}/V_{cmax} (Eqn 6) similarly derived from independent isotope and
413 environmental variables provided a good fit to the gas exchange estimate (Fig. 6) although the
414 modelled ratios were generally higher – both ratios estimated at the prevailing temperature. For
415 C_3 species average J_{max}/V_{cmax} ratios of around 2.0 are widely reported (e.g. Wullschleger, 1993),
416 but the model yielded many higher ratios (approaching 4.0 for the winter visit to Warra) and this
417 was related to cooler growth temperatures for certain sites and seasons – consistent with both
418 experimental evidence (Kattge & Knorr, 2007) and predictions (Wang *et al.*, 2017b). J_{max}/V_{cmax}
419 ratios inferred from gas exchange measurements confirmed a strong negative dependency on leaf
420 temperature, approaching unity as leaf temperatures neared 35°C (Supporting Information Fig.
421 S7).

422

423

Discussion

Theoretical optimality approaches permit prediction of photosynthetic parameters for species and ecosystems for which few or no empirical data are available, but of course such hypotheses require validation across as broad an environmental scale as possible. For diverse plant species growing at contrasting sites across Australia we show that leaf physiological parameters key to many Earth system models (ESMs) are predictable, to first order, using readily available environmental variables. Collectively, our findings support the contention that there now exists a unifying theoretical basis that ESMs can exploit to predict key leaf parameters across diverse species and biomes (Wang *et al.*, 2017b).

The unified stomatal model

It is often assumed that estimates of the same parameter obtained using different methods should match (e.g. Quentin *et al.*, 2015), but we found only weak agreement between our two versions of g_1. Although the underlying patterns of variation were similar for both bases, the poor correlation prompts the question which is the more reliable or informative. Our gas-exchange protocol was designed primarily to provide an instantaneous estimate of photosynthetic capacity. It may be that for many of these species xylem performance was compromised by the act of cutting the branches and hence water transport to the leaves was disrupted causing a reduction in g_s (Santiago & Mulkey, 2003). By contrast, g_1 values derived from the isotopic composition of leaf biomass reflect the growth environment as integrated over the leaf's development. In addition, metabolic processes post photosynthetic fixation create further fractionation steps that may cause Δ (hence χ and g_1) derived from leaf material to differ from instantaneous estimates (Cernusak *et al.*, 2013).

A recent study by Medlyn *et al.* (2017) compared g_1 estimates derived from three different datasets: gas exchange, leaf isotope (as here) and eddy covariance. They found that the three g_1 estimates were inconsistent, but in contrast to our results values for $g_{1\text{-isotope}}$ were generally lower than $g_{1\text{-leaf}}$ for a given PFT. Our own study is heavily dominated by evergreen broad leaf trees (47 of 50 species, Supporting Information Table S1), a classification that straddles three of the PFTs adopted in the Medlyn *et al.* study. For those three PFTs and shrubs (also represented here), Medlyn *et al.* (2017) reported significant differences between $g_{1\text{-leaf}}$ and $g_{1\text{-isotope}}$ values only for the savanna plants; the authors ascribe high variability in $g_{1\text{-leaf}}$ for savanna trees to marked seasonal differences. Their meta-analysis, however, included measurements from savannas in the seasonally dry tropics where monthly rainfall can vary by hundreds of mm (see for example Fig. 1 in Eamus *et al.*, 2000). The g_1 parameter is inversely proportional to the plant's intrinsic water

use efficiency (defined as A/g_s) and we expected to find inter-site differences that followed a gradient of moisture availability. Instead differences emerged only between the temperate forest at Warra and the moist tropical forests in FNQ. In a global study of 314 species at 56 sites, Lin *et al.* (2015) found no difference in g_1 among C_3 plants from temperate or tropical biomes, but did find important differences among PFTs: tropical moist forest trees at 3.37, shrubs at 4.22 and evergreen savanna trees at 7.18. Compared to the Lin *et al.* study, our tropical forest results are roughly double, whilst our g_1 values for the arid sites, derived in part from evergreen savanna trees, are much lower. Those lower g_1 estimates reported here (Fig. 2) arguably conform better to expectations of higher WUE in the dry conditions of those arid sites.

Stomatal behaviour must, in part, depend on environmental conditions, but we found no evidence of a seasonal effect on values of g_1. Lack of a seasonal response might be expected for moist tropical forests where the *T* and *D* differentials of wet *versus* dry seasons are much less pronounced than the summer *versus* winter contrasts of mid-latitude sites (Table 2) (Buchmann *et al.*, 1997). Surprisingly our results showed no relationship between g_1 and indices of water availability. In another Australian study of five evergreen eucalypt species growing at three sites along a rainfall gradient in the Northern Territory, Eamus *et al.* (2000) found no seasonal differences in transpiration rates despite marked seasonality in rainfall, aridity and leaf water potential. The authors propose that for these savanna trees, water use is determined by the limiting dry season conditions.

Our results showed poor consistency between the gas-exchange and isotope methods of estimating optimal stomatal behaviour. We found that the g_1 parameter of WUE was weakly influenced by air temperature over broad scales, but locally was at once widely variable among co-occurring species and conserved across changing seasons.

Predicting the ratio of leaf internal to ambient [CO_2]

A large body of work from the 1980s onwards has shown that ^{13}C discrimination is a reliable proxy for time-averaged χ (see Methods). Our results lend support to the model presented by Wang *et al.* (2017b) and show that isotope-derived χ is closely correlated to the corresponding value predicted from climate variables of growth *T* and *D*. In contrast to the original study, however, we found that the isotope-derived ratios were consistently higher than those produced by the model. Departing from the original study, we have applied an extended formulation of ^{13}C fractionation (Eqn 12); the ternary and photorespiration corrections here are relatively minor and act as partial offsets and so the principal disparity stems from our treatment of mesophyll conductance. Current ESMs, and the standard implementation of the FvCB model, ignore the

limitation placed on photosynthesis by g_m. In this study we adopted a single empirical correlation for estimating the drawdown from C_i to C_c (Eqn 9), but this is inevitably an oversimplification. Despite difficulties in measurement, g_m is known to vary among species and in response to environmental conditions (Flexas *et al.*, 2008; von Caemmerer & Evans, 2015). Importantly, ^{13}C discrimination methods can be combined with gas exchange measurements to provide estimates of g_m (Cernusak *et al.*, 2013). This is an important area for future research, both empirical and theoretical, on the control of photosynthetic traits although debate remains as to the necessity of incorporating g_m estimates into wider models (e.g. Bahar *et al.*, 2018).

Fitting the Wang *et al.* model to our data gave a coefficient of determination very similar to the original study (R^2 of 0.41 *versus* 0.39), but the fit was improved if the two seasons were treated separately (Table 3). One might expect seasonal contrasts to be captured by a stomatal model that specifies T and D as explanatory variables, but we found that their relative importance altered seasonally. In the favourable growing season, χ was more strongly influenced by variation in daytime T, but in the unfavourable season the primacy shifted to D. Greater influence for D under drier conditions is supported by a seasonal comparison of ecosystem WUE at the Alice Mulga site, where the response to D was more pronounced in the dry (winter) than the wet season linked to contrasting levels and variability of soil moisture content in the two seasons (Eamus *et al.*, 2013).

Offset notwithstanding, the implication of our results is that we now have a means of estimating C_i for modelling purposes. For this Australian study, where none of the sites sat higher than 750 m above sea level, we have ignored altitude effects on χ that are included in the original formulation (Eqn 4). Further studies could usefully test the model along a gradient encompassing a wider range of altitudes.

Photosynthetic parameters from first principles

Whilst our predictions of key parameters provided generally good agreement with gas exchange values, several discrepancies emerged. For a given site and season, the species-averaged V_{cmax} rates inferred from our gas-exchange measurements showed wide variation. Such variability amongst co-occurring species is to be expected (e.g. Bloomfield *et al.*, 2018) and likely reflects factors such as canopy position, and therefore light environment, and VPD. Our model performed less successfully when rates were normalised to the standard reference temperature of 25°C. The weaker correlation here may be partially explained by the underlying differentials in temperature offset from the common reference (see above): leaf temperature *versus* daytime averages. One effect of standardising the rates to a common reference temperature was to

narrow their range: inferred and modelled. Despite this contraction, the spectrum of site averages indicated higher rates for the species growing in arid conditions. When our inferred V_{cmax25} rates were modelled as a function of the light, T and χ variables underpinning Eqn 5, the residuals showed no discernible pattern with leaf mass per unit area (data not shown); suggesting that variation in leaf morphology (at a coarse scale) provided little explanatory power beyond these environmental variables.

What might be missing from our V_{cmax} model? In adopting a universal extinction coefficient (recognising that not all leaves display perpendicular to the sun's rays) and a leaf PAR estimate averaged for each plot (seasonal LAI values were adopted where available), our V_{cmax} model assumed a uniform light environment for all leaves (Eqn 8). One of the major difficulties is that we know very little about the light environments for these species. That quandary extends to our gas-exchange measurements, which employed a single saturating light setting across the study, and is likely one of the key reasons for the wide within-site variation in inferred V_{cmax} values. It has, however, been demonstrated that within-canopy gradients of photosynthetic capacity and light are not strictly proportional (e.g. Lloyd *et al.*, 2010) e.g. leaves in poor light appear to have superfluous capacity thus breaching the optimality hypothesis. From our own results it is not apparent that the model performed differently for those sites (Daintree and Cumberland Plain) where we sampled tree branches from the gondola of a crane and where we might have expected the light-averaging step to produce an underestimate. In considering why optimal canopies are not observed in nature, Niinemets (2012) proposed a series of additional constraints or mechanisms including leaf construction, acclimation and light-competition.

Even more challenging is the possibility that rates of photosynthesis are driven by the plant's requirements for photosynthate (buffered by existing stores) rather than what is possible or optimal. The demands - spanning respiration, reproduction, defence, exudates – represent a complex network of plant processes intimately connected to the surrounding biotic and abiotic environment and subject to stochastic fluctuation. The different timescales operating for our two V_{cmax} estimates create the likelihood of quite distinct underlying phenology and sink demand.

Changes or differences in growth temperature are expected to require adjustment in the plant's photosynthetic apparatus, often manifested as variation in the J_{max}/V_{cmax} ratio. Accordingly, we found elevated ratios related to the cooler seasons and sites reflecting the ratio's negative dependence on temperature (Fig. 6). Our gas exchange data suggested a strong negative linear relationship with leaf temperature (Supporting Information Fig. S7), but with a steeper slope (-

0.08 *versus* -0.035 °C^{-1}) than that reported by Kattge & Knorr (2007). Our model (Eqn 6) predicted J_{max}/V_{cmax} ratios that were consistently higher than those inferred from the gas exchange measurements and that coincides with the elevated $\chi_{isotope}$ values described above: the modelled J_{max}/V_{cmax} ratio increasing with C_i.

Concluding remarks

We have used our unique dataset to test predictions of leaf photosynthetic traits across a range of climates and plant species. Demonstrating the validity of these predictions has application for the ESM community. Current ESMs are still hampered by uncertainty, much of which relates to incomplete or inaccurate representations of the fundamental processes that govern carbon fixation at the leaf, canopy and ecosystem levels. The path forward will involve sustained efforts both to formulate explicit, unifying theories about the control of these processes and to test and refine them with the help of field measurements. This research represents a step along that path.

Acknowledgments

TERN (http://www.tern.org.au) is supported by the Australian Government through the National Collaborative Infrastructure Strategy (NCRIS). This work was specifically facilitated through a Supplemental Grant to TERN's eMAST and SuperSites facilities. The support of the Australian Research Council to OKA (DP130101252 and CE140100008) and DE (DP140101150) is also acknowledged. This work is a contribution to the AXA Chair Programme in Biosphere and Climate Impacts and the Imperial College initiative on Grand Challenges in Ecosystems and the Environment. KJB was hosted during the writing of this manuscript by the University of Exeter.

Author contributions

ICP, OKA and KJB designed the study. DE, DSE, MMB, PC, JC, MJL, CM, WSM, TW and IJW co-ordinated site access, species identification and logistical support. KJB, JJGE, LSH,

HFT and LZ conducted fieldwork. BJE, MFH and MJL helped to compile the climate data. RR conducted the isotope analysis and LAC proposed the extended discrimination model (Eqn 12). BEM guided calculation of the g_1 parameter. KJB led the analysis of the data and wrote the manuscript with input from all authors.

References

Ali AA, Xu CG, Rogers A, McDowell NG, Medlyn BE, Fisher RA, Wullschleger SD, Reich PB, Vrugt JA, Bauerle WL, et al. 2015. Global-scale environmental control of plant photosynthetic capacity. *Ecological Applications* **25**(8): 2349-2365.

Ayub G, Smith RA, Tissue DT, Atkin OK. 2011. Impacts of drought on leaf respiration in darkness and light in *Eucalyptus saligna* exposed to industrial-age atmospheric CO_2 and growth temperature. *New Phytologist* **190**(4): 1003-1018.

Badger MR, Collatz GJ. 1977. Studies on the kinetic mechanism of ribulose-1, 5-bisphosphate carboxylase and oxygenase reactions, with particular reference to the effect of temperature on kinetic parameters. *Carnegie Institute of Washington Yearbook* **76**: 355-361.

Bahar NHA, Hayes L, Scafaro AP, Atkin OK, Evans JR. 2018. Mesophyll conductance does not contribute to greater photosynthetic rate per unit nitrogen in temperate compared with tropical evergreen wet-forest tree leaves. *New Phytologist* **218**(2): 492-505.

Beringer J, Hutley LB, McHugh I, Arndt SK, Campbell D, Cleugh HA, Cleverly J, Resco de Dios V, Eamus D, Evans B, et al. 2016. An introduction to the Australian and New Zealand flux tower network - OzFlux. *Biogeosciences Discuss.* **2016**: 1-52.

Bernacchi CJ, Singsaas EL, Pimentel C, Portis AR, Long SP. 2001. Improved temperature response functions for models of Rubisco-limited photosynthesis. *Plant Cell and Environment* **24**(2): 253-259.

Bloomfield KJ, Cernusak LA, Eamus D, Ellsworth DS, Prentice IC, Wright IJ, Boer M, Bradford MG, Cale P, Cleverly J, et al. 2018. A continental-scale assessment of variability in leaf traits: within species, across sites and between seasons. *Functional Ecology* **32**(6): 1492-1506.

Breheny P, Burchett W. 2017. Visualization of regression models using visreg. *The R Journal* **9**(2): 56-71.

Britton CM, Dodd JD. 1976. Relationships of photosynthetically active radiation and shortwave irradiance. *Agricultural Meteorology* **17**(1): 1-7.

Buchmann N, Guehl JM, Barigah TS, Ehleringer JR. 1997. Interseasonal comparison of CO_2 concentrations, isotopic composition, and carbon dynamics in an Amazonian rainforest (French Guiana). *Oecologia* **110**(1): 120-131.

Cernusak LA, Ubierna N, Winter K, Holtum JAM, Marshall JD, Farquhar GD. 2013. Environmental and physiological determinants of carbon isotope discrimination in terrestrial plants. *New Phytologist* **200**(4): 950-965.

Chen JL, Reynolds JF, Harley PC, Tenhunen JD. 1993. Coordination theory of leaf nitrogen distribution in a canopy. *Oecologia* **93**(1): 63-69.

Collatz GJ, Ball JT, Grivet C, Berry JA. 1991. Physiological and environmental regulation of stomatal conductance, photosynthesis and transpiration: a model that includes a laminar boundary layer. *Agricultural and Forest Meteorology* **54**(2-4): 107-136.

Cowan IR, Farquhar GD 1977. Stomatal function in relation to leaf metabolism and environment. In: Jennings DH ed. *Integration of Activity in Higher Plants*. Cambridge: Cambridge University Press, 471-505.

De Kauwe MG, Lin YS, Wright IJ, Medlyn BE, Crous KY, Ellsworth DS, Maire V, Prentice IC, Atkin OK, Rogers A, et al. 2016. A test of the 'one-point method' for estimating maximum carboxylation capacity from field-measured, light-saturated photosynthesis. *New Phytologist* **210**(3): 1130-1144.

Dewar R, Mauranen A, Mäkelä A, Hölttä T, Medlyn B, Vesala T. 2018. New insights into the covariation of stomatal, mesophyll and hydraulic conductances from optimization models incorporating nonstomatal limitations to photosynthesis. *New Phytologist* **217**(2): 571-585.

Domingues TF, Meir P, Feldpausch TR, Saiz G, Veenendaal EM, Schrodt F, Bird M, Djagbletey G, Hien F, Compaore H, et al. 2010. Co-limitation of photosynthetic capacity by nitrogen and phosphorus in West Africa woodlands. *Plant Cell and Environment* **33**(6): 959-980.

Dong N, Prentice IC, Evans BJ, Caddy-Retalic S, Lowe AJ, Wright IJ. 2017. Leaf nitrogen from first principles: field evidence for adaptive variation with climate. *Biogeosciences* **14**(2): 481-495.

Duursma RA. 2015. plantecophys - an R package for analysing and modelling leaf gas exchange data. *Plos One* **10**(11).

Eamus D, Cleverly J, Boulain N, Grant N, Faux R, Villalobos-Vega R. 2013. Carbon and water fluxes in an arid-zone *Acacia* savanna woodland: An analyses of seasonal patterns and responses to rainfall events. *Agricultural and Forest Meteorology* **182**: 225-238.

Eamus D, O'Grady AP, Hutley L. 2000. Dry season conditions determine wet season water use in the wet-dry tropical savannas of northern Australia. *Tree Physiology* **20**(18): 1219-1226.

Evans JR, von Caemmerer S. 1996. Carbon dioxide diffusion inside leaves. *Plant Physiology* **110**(2): 339-346.

Farquhar GD, Cernusak LA. 2012. Ternary effects on the gas exchange of isotopologues of carbon dioxide. *Plant Cell and Environment* **35**(7): 1221-1231.

Farquhar GD, Ehleringer JR, Hubick KT. 1989. Carbon isotope discrimination and photosynthesis. *Annual Review of Plant Physiology and Plant Molecular Biology* **40**: 503-537.

Farquhar GD, O'Leary MH, Berry JA. 1982. On the relationship between carbon isotope discrimination and the inter-cellular carbon dioxide concentration in leaves. *Australian Journal of Plant Physiology* **9**(2): 121-137.

Farquhar GD, von Caemmerer S, Berry JA. 1980. A biochemical model of photosynthetic CO_2 assimilation in leaves of C_3 species. *Planta* **149**: 78-90.

Flexas J, Ribas-Carbo M, Diaz-Espejo A, Galmes J, Medrano H. 2008. Mesophyll conductance to CO_2: current knowledge and future prospects. *Plant Cell and Environment* **31**(5): 602-621.

Hutchinson MF, McKenney DW, Lawrence K, Pedlar JH, Hopkinson RF, Milewska E, Papadopol P. 2009. Development and testing of Canada-wide interpolated spatial models of daily minimum-maximum temperature and precipitation for 1961-2003. *Journal of Applied Meteorology and Climatology* **48**(4): 725-741.

Karan M, Liddell M, Prober SM, Arndt S, Beringer J, Boer M, Cleverly J, Eamus D, Grace P, Van Gorsel E, et al. 2016. The Australian SuperSite Network: A continental,

long-term terrestrial ecosystem observatory. *Science of the Total Environment* **568**: 1263-1274.

Kattge J, Knorr W. 2007. Temperature acclimation in a biochemical model of photosynthesis: a reanalysis of data from 36 species. *Plant Cell and Environment* **30**(9): 1176-1190.

Katul G, Manzoni S, Palmroth S, Oren R. 2010. A stomatal optimization theory to describe the effects of atmospheric CO_2 on leaf photosynthesis and transpiration. *Annals of Botany* **105**(3): 431-442.

Kitajima K, Mulkey SS, Wright SJ. 2005. Variation in crown light utilization characteristics among tropical canopy trees. *Annals of Botany* **95**(3): 535-547.

Lambers H, Chapin FS, Pons TL. 2008. *Plant Physiological Ecology*: Springer New York.

Lin YS, Medlyn BE, Duursma RA, Prentice IC, Wang H, Baig S, Eamus D, de Dios VR, Mitchell P, Ellsworth DS, et al. 2015. Optimal stomatal behaviour around the world. *Nature Climate Change* **5**(5): 459-464.

Lloyd J. 1991. Modeling stomatal responses to environment in *Macadamia integrifolia*. *Australian Journal of Plant Physiology* **18**(6): 649-660.

Lloyd J, Patiño S, Paiva RQ, Nardoto GB, Quesada CA, Santos AJB, Baker TR, Brand WA, Hilke I, Gielmann H, et al. 2010. Optimisation of photosynthetic carbon gain and within-canopy gradients of associated foliar traits for Amazon forest trees. *Biogeosciences* **7**(6): 1833-1859.

Maire V, Martre P, Kattge J, Gastal F, Esser G, Fontaine S, Soussana JF. 2012. The coordination of leaf photosynthesis links C and N fluxes in C_3 plant species. *Plos One* **7**(6).

Mäkelä A, Givnish TJ, Berninger F, Buckley TN, Farquhar GD, Hari P. 2002. Challenges and opportunities of the optimality approach in plant ecology. *Silva Fennica* **36**(3): 605-614.

Medlyn BE, De Kauwe MG, Lin Y-S, Knauer J, Duursma RA, Williams CA, Arneth A, Clement R, Isaac P, Limousin J-M, et al. 2017. How do leaf and ecosystem measures of water-use efficiency compare? *New Phytologist* **216**(3): 758-770.

Medlyn BE, Dreyer E, Ellsworth D, Forstreuter M, Harley PC, Kirschbaum MUF, Le Roux X, Montpied P, Strassemeyer J, Walcroft A, et al. 2002. Temperature response

of parameters of a biochemically based model of photosynthesis. II. A review of experimental data. *Plant Cell and Environment* **25**(9): 1167-1179.

Medlyn BE, Duursma RA, De Kauwe MG, Prentice IC. 2013. The optimal stomatal response to atmospheric CO_2 concentration: Alternative solutions, alternative interpretations. *Agricultural and Forest Meteorology* **182**: 200-203.

Medlyn BE, Duursma RA, Eamus D, Ellsworth DS, Prentice IC, Barton CVM, Crous KY, de Angelis P, Freeman M, Wingate L. 2011. Reconciling the optimal and empirical approaches to modelling stomatal conductance. *Global Change Biology* **17**(6): 2134-2144.

Niinemets U. 2012. Optimization of foliage photosynthetic capacity in tree canopies: towards identifying missing constraints. *Tree Physiology* **32**(5): 505-509.

Niinemets U, Diaz-Espejo A, Flexas J, Galmes J, Warren CR. 2009. Role of mesophyll diffusion conductance in constraining potential photosynthetic productivity in the field. *Journal of Experimental Botany* **60**(8): 2249-2270.

Pinheiro J, Bates D, DebRoy S, Sarkar D, R Core Team 2018. nlme: linear and nonlinear mixed effects models. https://CRAN.R-project.org/package=nlme.

Poorter H, Evans JR. 1998. Photosynthetic nitrogen-use efficiency of species that differ inherently in specific leaf area. *Oecologia* **116**(1-2): 26-37.

Prentice IC, Dong N, Gleason SM, Maire V, Wright IJ. 2014. Balancing the costs of carbon gain and water transport: testing a new theoretical framework for plant functional ecology. *Ecology Letters* **17**(1): 82-91.

Prentice IC, Liang X, Medlyn BE, Wang YP. 2015. Reliable, robust and realistic: the three Rs of next-generation land-surface modelling. *Atmospheric Chemistry and Physics* **15**(10): 5987-6005.

Quentin AG, Pinkard EA, Ryan MG, Tissue DT, Baggett LS, Adams HD, Maillard P, Marchand J, Landhausser SM, Lacointe A, et al. 2015. Non-structural carbohydrates in woody plants compared among laboratories. *Tree Physiology* **35**(11): 1146-1165.

R Development Core Team 2017. R: A language and environment for statistical computing. Vienna, Austria: R Foundation for Statistical Computing. https://www.R-project.org/.

Read J, Farquhar G. 1991. Comparative studies in *Nothofagus* (Fagaceae). 1. Leaf carbon isotope discrimination. *Functional Ecology* **5**(5): 684-695.

Reich PB, Wright IJ, Lusk CH. 2007. Predicting leaf physiology from simple plant and climate attributes: A global GLOPNET analysis. *Ecological Applications* **17**(7): 1982-1988.

Rogers A. 2014. The use and misuse of $V_{c,max}$ in Earth system models. *Photosynthesis Research* **119**(1-2): 15-29.

Rumman R, Atkin OK, Bloomfield KJ, Eamus D. 2018. Variation in bulk-leaf ^{13}C discrimination, leaf traits and water-use efficiency-trait relationships along a continental-scale climate gradient in Australia. *Global Change Biology* **24**(3): 1186-1200.

Santiago LS, Mulkey SS. 2003. A test of gas exchange measurements on excised canopy branches of ten tropical tree species. *Photosynthetica* **41**(3): 343-347.

Schulze ED, Kelliher FM, Körner C, Lloyd J, Leuning R. 1994. Relationships among maximum stomatal conductance, ecosystem surface conductance, carbon assimilation rate and plant nitrogen nutrition: a global ecology scaling exercise. *Annual Review of Ecology and Systematics* **25**: 629-660.

Seibt U, Rajabi A, Griffiths H, Berry JA. 2008. Carbon isotopes and water use efficiency: sense and sensitivity. *Oecologia* **155**(3): 441-454.

Sperry JS, Wang YJ, Wolfe BT, Mackay DS, Anderegg WRL, McDowell NG, Pockman WT. 2016. Pragmatic hydraulic theory predicts stomatal responses to climatic water deficits. *New Phytologist* **212**(3): 577-589.

Thomas DS, Eamus D, Bell D. 1999. Optimization theory of stomatal behaviour - II. Stomatal responses of several tree species of north Australia to changes in light, soil and atmospheric water content and temperature. *Journal of Experimental Botany* **50**(332): 393-400.

Ubierna N, Farquhar GD. 2014. Advances in measurements and models of photosynthetic carbon isotope discrimination in C_3 plants. *Plant Cell and Environment* **37**(7): 1494-1498.

Verheijen LM, Brovkin V, Aerts R, Bonisch G, Cornelissen JHC, Kattge J, Reich PB, Wright IJ, van Bodegom PM. 2013. Impacts of trait variation through observed trait-climate relationships on performance of an Earth system model: a conceptual analysis. *Biogeosciences* **10**(8): 5497-5515.

von Caemmerer S, Evans JR. 2015. Temperature responses of mesophyll conductance differ greatly between species. *Plant Cell and Environment* **38**(4): 629-637.

von Caemmerer S, Evans JR, Hudson GS, Andrews TJ. 1994. The kinetics of ribulose-1,5-bisphosphate carboxylase/oxygenase in vivo inferred from measurements of photosynthesis in leaves of transgenic tobacco. *Planta* **195**(1): 88-97.

Wang H, Prentice IC, Davis TW, Keenan TF, Wright IJ, Peng CH. 2017a. Photosynthetic responses to altitude: an explanation based on optimality principles. *New Phytologist* **213**(3): 976-982.

Wang H, Prentice IC, Keenan TF, Davis TW, Wright IJ, Cornwell WK, Evans BJ, Peng CH. 2017b. Towards a universal model for carbon dioxide uptake by plants. *Nature Plants* **3**(9): 734-741.

Wolf A, Anderegg WRL, Pacala SW. 2016. Optimal stomatal behavior with competition for water and risk of hydraulic impairment. *Proceedings of the National Academy of Sciences of the United States of America* **113**(46): E7222-E7230.

Wong SC, Cowan IR, Farquhar GD. 1979. Stomatal conductance correlates with photosynthetic capacity. *Nature* **282**(5737): 424-426.

Wright IJ, Reich PB, Westoby M, Ackerly DD, Baruch Z, Bongers F, Cavender-Bares J, Chapin T, Cornelissen JHC, Diemer M, et al. 2004. The worldwide leaf economics spectrum. *Nature* **428**(6985): 821-827.

Wullschleger SD. 1993. Biochemical limitations to carbon assimilation in C_3 plants - a retrospective analysis of A/C_i curves from 109 species. *Journal of Experimental Botany* **44**(262): 907-920.

Supporting Information

Fig. S1 Map and key climate indicators for each of the study sites.

Fig. S2 Instantaneous chamber conditions *versus* time-averaged equivalents.

Fig. S3 Parameter $g_{1\_isotope}$ as a function of air temperature.

Fig. S4 Comparison of key parameters adopting 'neo-classical' and 'simple' fractionation.

Fig. S5 The effect of measurement temperature differentials on normalised rates of $V_{cmax.}$

Fig. S6 Temperature dependence of the V_{cmax} model Eqn 5.

Fig. S7 Temperature dependence of the J_{max} : V_{cmax} ratio.

Table S1 Plant species by site.

Table S2 Leaf gas-exchange traits averaged by Site_Season_Species.

790

791

792 **Table 1** Site location and descriptors.

793

794 The sites are listed in order of increasing absolute latitude. An Australian map with the site locations indicated is included in Supporting Information Fig. S1. Leaf area
795 index is the ratio of projected leaf to ground surface area. Climate indices are annual long-term averages of interpolated data obtained from the Terrestrial Ecosystem
796 Research Network (TERN) eMAST facility. Moisture index is shown as the ratio of precipitation to potential evapotranspiration. Additional details for each site may be
797 found on the TERN SuperSite website (www.supersites.net.au). asl, above sea level; Leaf N, leaf nitrogen; Leaf P, leaf phosphorus.

798

Table 2 Climate conditions for each campaign (Site_Season) for the 90 d period ending on the final day of fieldwork.

Air temperature (Ta), precipitation, net radiation (Fn), vapour pressure deficit (VPD), soil water fraction (Sws, top layer), short-wave down-welling radiation (Fsd). Rainfall figures are totals, other values are means; temperature, radiation and VPD figures relate to daylight hours only. In most cases the climate data have been obtained from instruments centred on flux towers located at each site and managed under the OzFlux network (**www.ozflux.org.au**). In three cases our fieldwork campaigns were made before the flux towers were fully operational and in these instances we have used interpolated 24 h data obtained from ANUClimate (**www.emast.org.au/our-infrastructure/observations/anuclimate_data/**). As we prepared the manuscript, daily radiation data for the periods of interest were not available within ANUClimate and so those radiation data have been obtained for the nearest automated weather station operated by the Australian Bureau of Meteorology (**www.bom.gov.au**). The designation of Favourable and Unfavourable seasons is based on a local assessment of growing conditions. na, not available.

Table 3 Linear model summaries, following Wang *et al*. (2017b) and Eqn 4: **i**n each case the response variable is the logit-transformed isotope-derived ratio of leaf internal to ambient CO_2 partial pressure (χ).

The explanatory variables are the difference in the mean air temperature for the preceding quarter from 25°C (ΔT, °C) and the natural logarithm of the mean vapour pressure deficit for the preceding quarter ($\log_e D$, kPa). The theoretical values are partial derivatives for each predictor, evaluated at 'standard' conditions (T=25°C, D=1 kPa). The *t*-test result is the probability of no difference between the fitted estimate and the theoretical value (null hypothesis). Separate model iterations were run for the complete data-set and then for each of the two seasons. na, not applicable.

Fig. 1 Relationship between two estimates of the g_1 parameter (Eqn 2) derived from: instantaneous gas exchange measurements ($g_{1\text{-leaf}}$) and leaf isotope discrimination ($g_{1\text{-isotope}}$). The points represent seasonal means for individual plant species and sites are differentiated by colour. The dashed line represents the ideal 1 : 1 fit. The *x*-axis has been restricted to exclude eight species (one Warra, five Robson Ck and two Daintree) with $g_{1\text{-isotope}}$ greater than 20 $kPa^{0.5}$.

Fig. 2 Boxplot showing the g_1 values estimated from leaf isotope discrimination grouped by site and including both seasons. The *y*-axis has been restricted to exclude eight species (one Warra, five Robson Ck and two Daintree) with $g_{1\text{-isotope}}$ greater than 20 $kPa^{0.5}$. The boxes indicate the interquartile range and median values.

Whiskers extend to the largest or smallest observation that fall within 1.5 times the box size; any observations outside these values are shown as individual points. Boxes which share the same letter denote site means that were not significantly different (Tukey's honest significant differences). The number of species included for each site is indicated. The inset plot shows the equivalent analysis for the parameter derived from instantaneous gas exchange measurements ($g_{1\text{-leaf}}$, notice that the scales of the axes differ).

Fig. 3 Values of χ (the ratio of leaf internal to ambient CO_2 partial pressure) obtained from ^{13}C isotope discrimination, Eqn 12 plotted against corresponding predicted values of χ based on environmental variables of temperature (T) and vapour pressure deficit (D) obtained from the OzFlux network, Eqn 4. Both estimates have been modified to account for mesophyll conductance. The large coloured dots represent the site means (combining all species and seasons) and the whiskers give the ± SD. The smaller dots represent underlying seasonal means for individual plant species (three to five plants per species). The dashed line represents the ideal 1 : 1 fit. The Pearson correlation indicated relates to the underlying species' means (smaller dots); the corresponding correlation based on site means (large dots) is 0.93.

Fig. 4 Partial residual plots showing the logit-transformed ratio of leaf internal to external CO_2 partial pressure (χ) derived from stable carbon isotope discrimination data as a function of time averaged environmental variables: air temperature and vapour pressure deficit (D). Separate panels are shown for the contrasting visits: (a, b) favourable season, (c, d) unfavourable season. Model coefficients and summaries appear in Table 3.

Fig. 5 Goodness of fit plot for the carboxylation (V_{cmax}) model Eqn 5 using C_i data derived from carbon isotope discrimination plotted against estimates inferred from independent gas exchange measurements. (a) Rates at the prevailing measurement temperature; (b) the corresponding plot with rates standardised to a common reference temperature of 25°C. The large coloured symbols represent the Site_Season means (combining all species) and the whiskers give the ± SD; the smaller dots represent underlying seasonal means for individual plant species (three to five plants per species). The dashed line represents the ideal 1 : 1 fit. The Pearson correlations indicated relate to the underlying species' means (smaller dots).

Fig. 6 Goodness of fit plot for the modelled ratio of electron transport to carboxylation capacity ($J_{max} : V_{cmax}$) from Eqn 6 using C_i data derived from carbon isotope discrimination plotted against independent gas exchange estimates – both ratios expressed at the prevailing temperature. The large coloured symbols represent the Site_Season means (combining all species) and the whiskers give the ± SD. The smaller dots represent underlying seasonal means for individual plant species (three to five plants per species). The dashed line

867 represents the ideal 1 : 1 fit. The Pearson correlation indicated relates to the underlying species' means (smaller
868 dots); the corresponding correlation based on Site_Season means (large symbols) is 0.86.

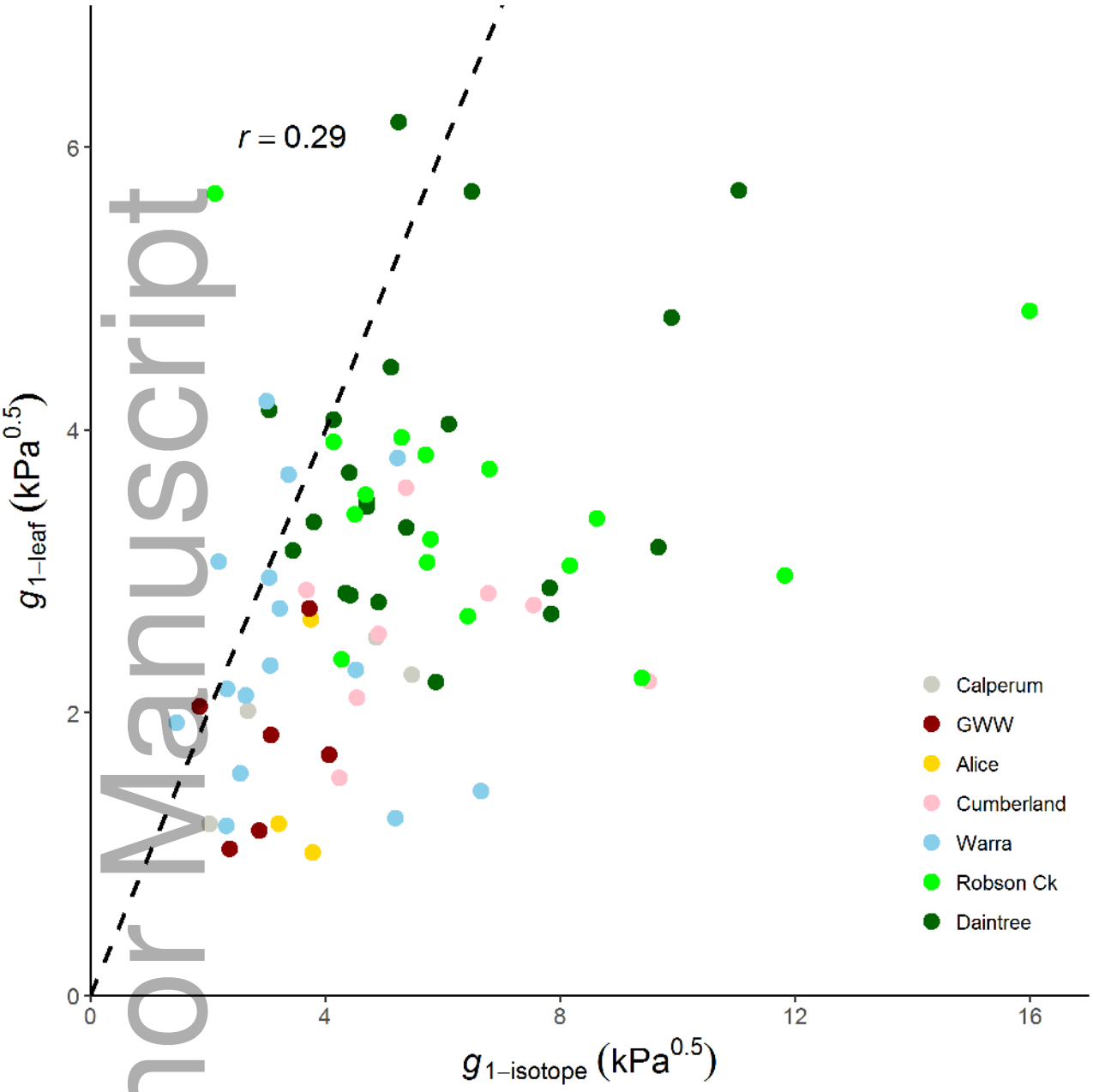

nph_15495_f1.tif

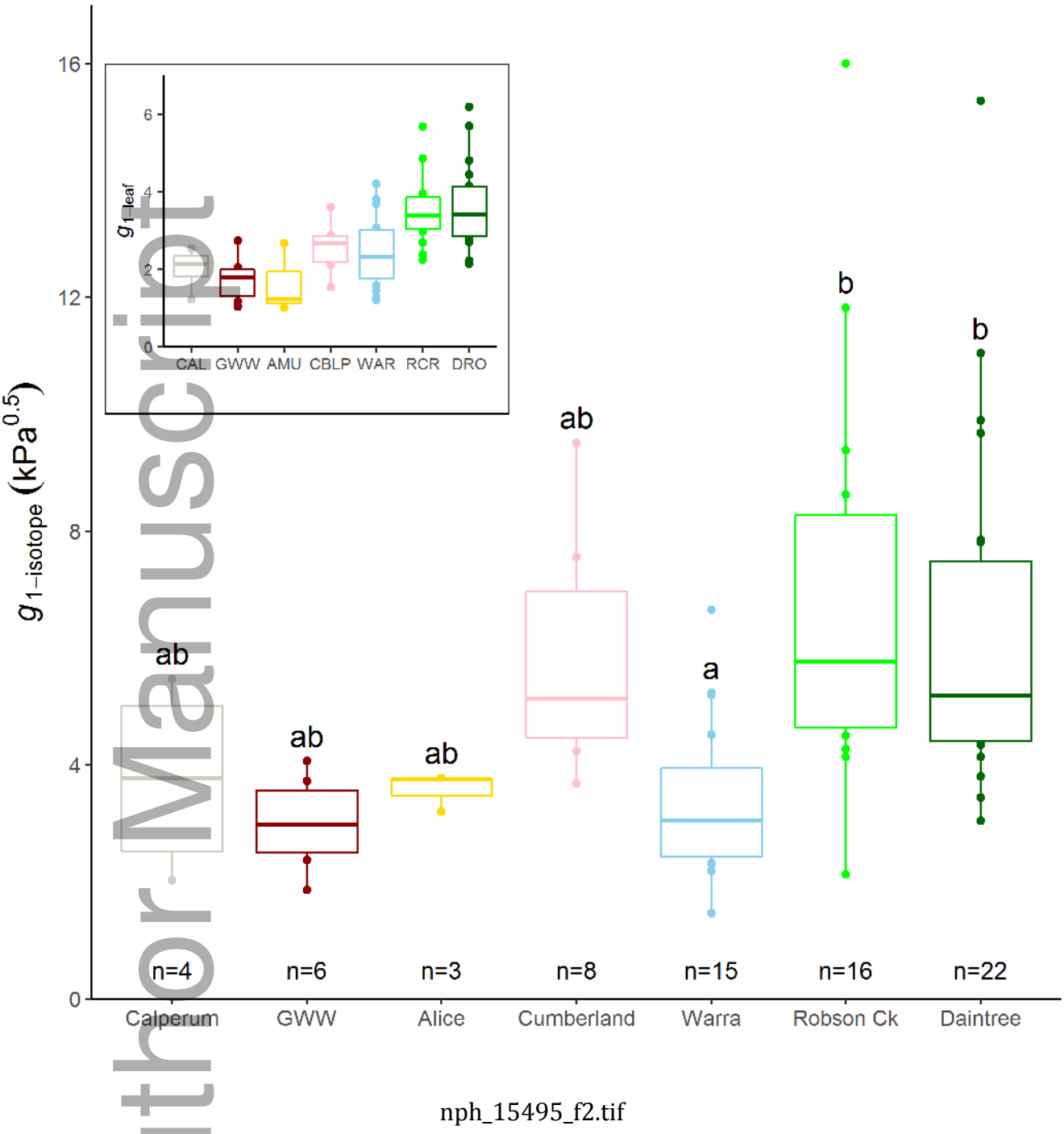

nph_15495_f2.tif

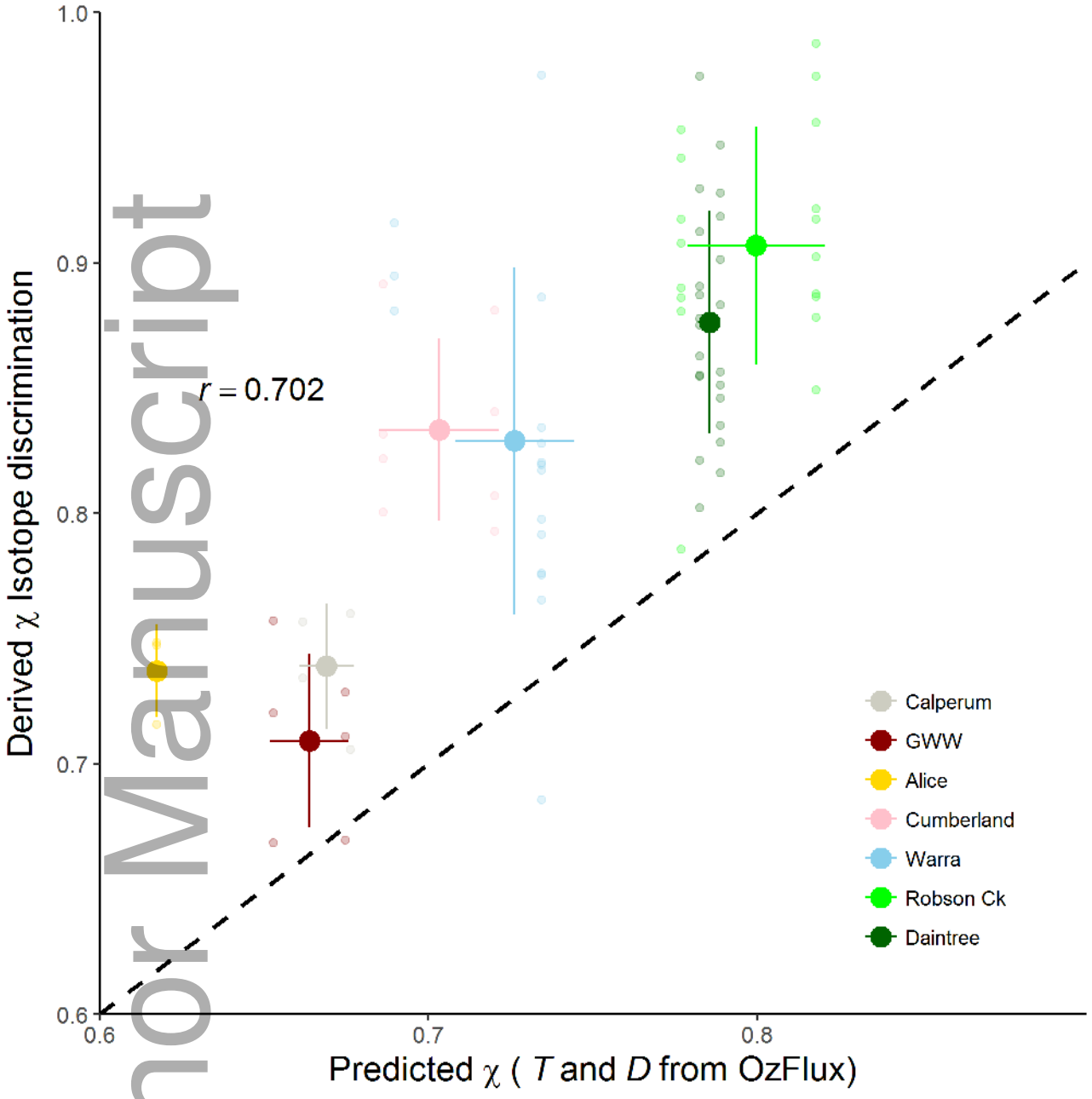

nph_15495_f3.tif

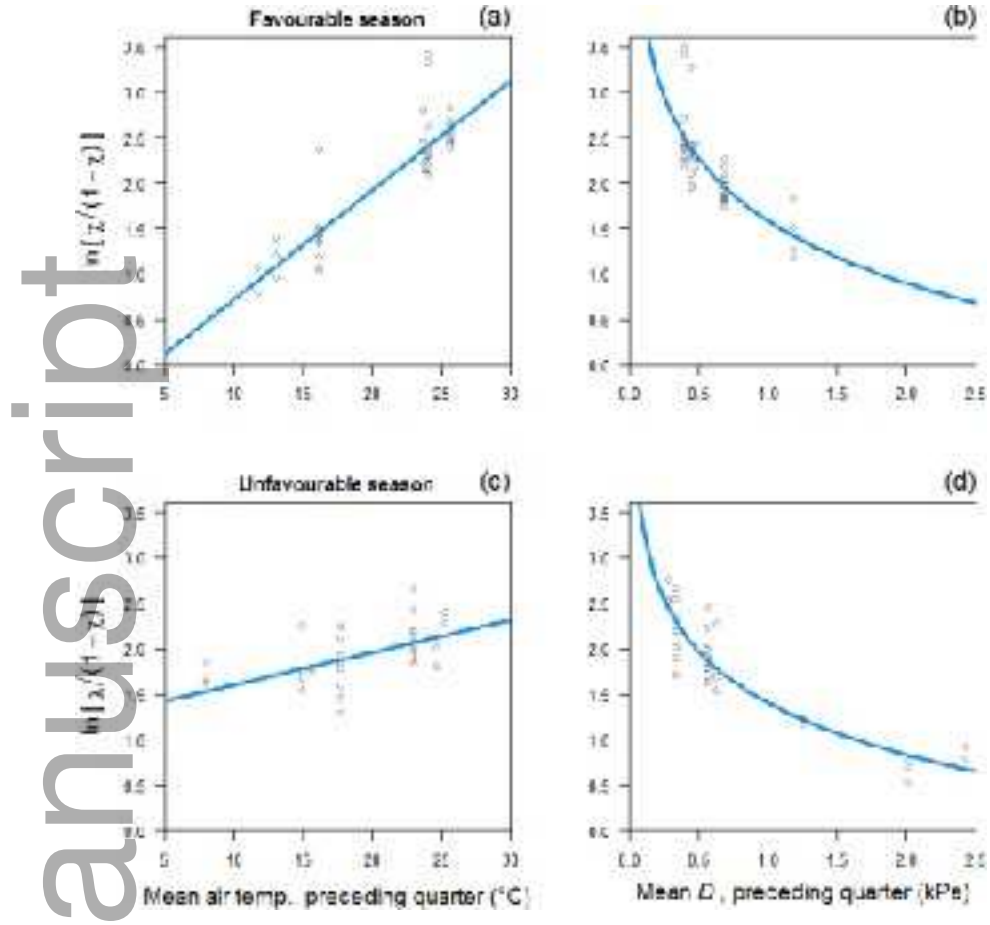

nph_15495_f4.tiff

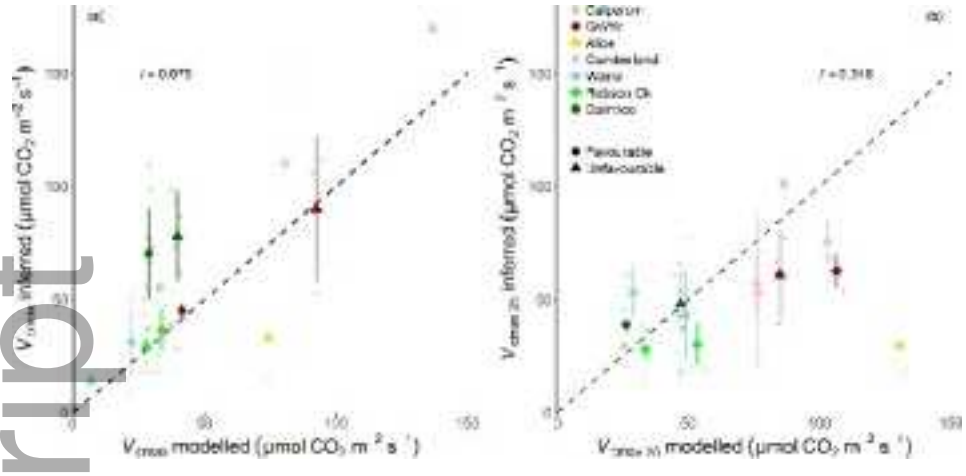

nph_15495_f5.tif

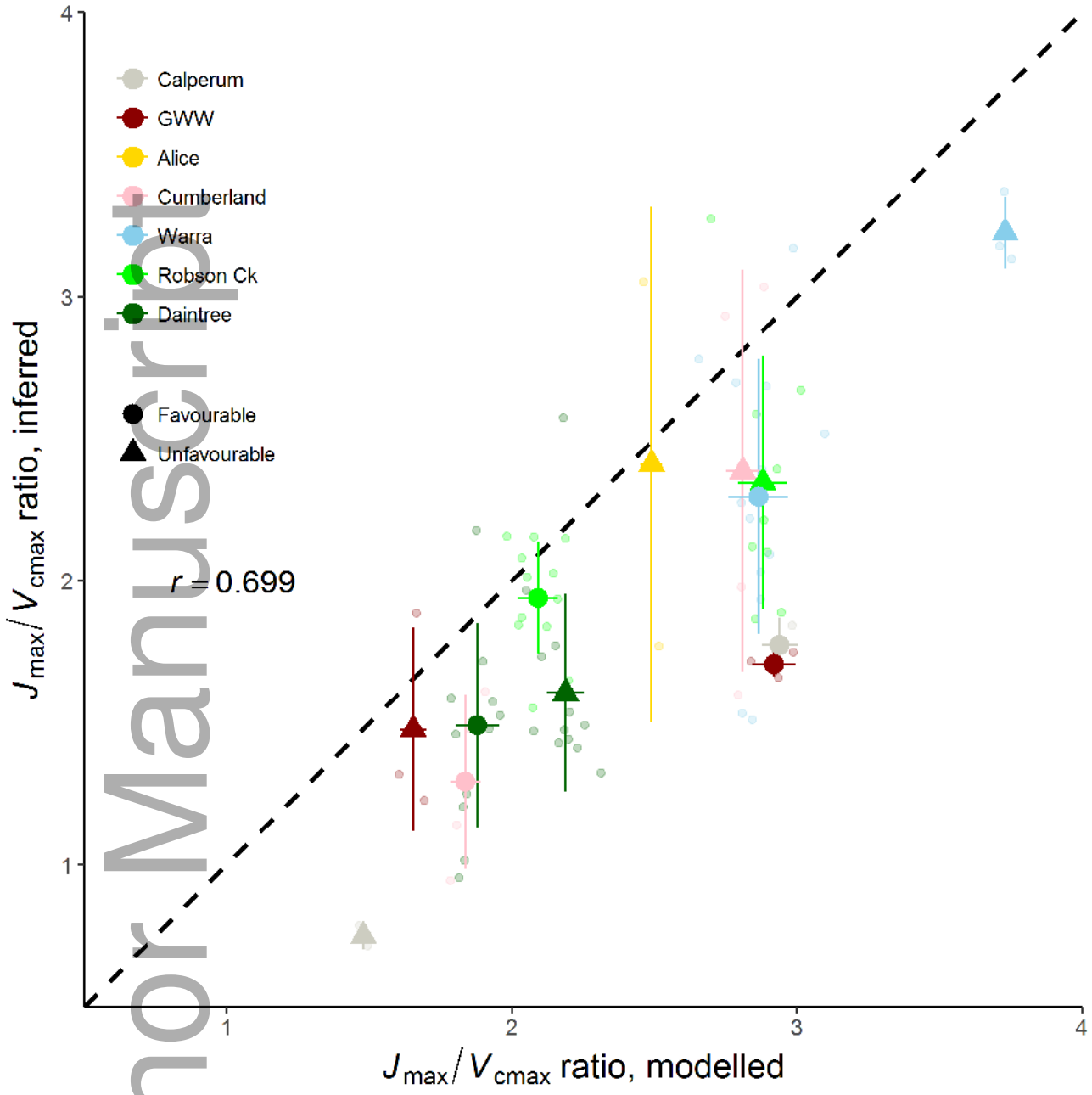

nph_15495_f6.tif